Earth Syst. Dynam. Discuss., 6, 1897–1937, 2015
www.earth-syst-dynam-discuss.net/6/1897/2015/
doi:10.5194/esdd-6-1897-2015

Earth System Dynamics
Discussions
Open Access

The role of spatial scale and background climate in the latitudinal temperature response to deforestation

Y. Li[1,2,3,4], N. de Noblet-Ducoudré[5], E. L. Davin[6], N. Zeng[2], S. Motesharrei[4,7,8], S. C. Li[1,3], and E. Kalnay[2,4]

[1]College of Urban and Environmental Sciences, Peking University, Beijing 100871, China
[2]Department of Atmospheric and Oceanic Science, University of Maryland, College Park, Maryland 20742, USA
[3]Key Laboratory for Earth Surface Processes of The Ministry of Education, Peking University, Beijing 100871, China
[4]The Institute for Physical Science and Technology, University of Maryland, College Park, Maryland 20742, USA
[5]Laboratoire des Sciences du Climat et de l'Environnement, Institut Pierre Simon Laplace, UMR8212, Gif-sur-Yvette, France
[6]Institute for Atmospheric and Climate Science, Eidgenössiche Technische Hochschule (ETH) Zurich, 8092 Zürich, Switzerland
[7]Department of Physics, University of Maryland, College Park, Maryland 20742, USA
[8]National Socio-Environmental Synthesis Center (SESYNC), Annapolis, Maryland, 21401, USA

Received: 5 September 2015 – Accepted: 16 September 2015 – Published: 9 October 2015

Correspondence to: Y. Li (yanli.geo@gmail.com)

Published by Copernicus Publications on behalf of the European Geosciences Union.

Abstract

Previous modeling and empirical studies have shown that the biophysical impact of deforestation is to warm the tropics and cool the extra-tropics. In this study, we use an earth system model to investigate how deforestation at various spatial scales affects ground temperature, with an emphasis on the latitudinal temperature response and its underlying mechanisms. Results show that the latitudinal pattern of temperature response depends non-linearly on the spatial extent of deforestation and the fraction of vegetation change. Compared with regional deforestation, temperature change in global deforestation is greatly amplified in temperate and boreal regions, but is dampened in tropical regions. Incremental forest removal leads to increasingly larger cooling in temperate and boreal regions, while the temperature increase saturates in tropical regions. The latitudinal and spatial patterns of the temperature response are driven by two processes with competing temperature effects: decreases in absorbed shortwave radiation due to increased albedo and decreases in evapotranspiration. These changes in the surface energy balance reflect the importance of the background climate on modifying the deforestation impact. Shortwave radiation and precipitation have an intrinsic geographical distribution that constrains the effects of biophysical changes and therefore leads to temperature changes that are spatially varying. For example, wet (dry) climate favors larger (smaller) evapotranspiration change, thus warming (cooling) is more likely to occur. Further analysis on the contribution of individual biophysical factors (albedo, roughness, and evapotranspiration efficiency) reveals that the latitudinal signature embodied in the temperature change probably result from the background climate conditions rather than the initial biophysical perturbation.

1 Introduction

Forests play a critical role in regulating climate via both biogeochemical and biophysical processes that can affect earth's radiation balance, hydrological cycle, and atmospheric

ESDD
6, 1897–1937, 2015

composition (Bonan, 2008). Driven by anthropogenic activities directly, e.g., agriculture expansion, or indirectly, e.g., climate change induced disturbance (Allen et al., 2010), deforestation is a major land conversion that had taken place historically over large scales and continues to be prevalent in the 21th century (Hansen et al., 2013). Compared with biogeochemical effects, i.e., release of CO_2 to the atmosphere that warms the global climate, biophysical effects are more heterogeneous, strongly felt at regional and local levels (Pitman et al., 2012), and vary with season and location (Snyder et al., 2004; Betts et al., 2007; Li et al., 2015).

An interesting characteristic of deforestation is the observed latitude dependency in the temperature response, confirmed by previous climate model studies. Large-scale deforestation in the tropics leads to a temperature increase (Nobre et al., 1991; Snyder et al., 2004) mostly due to a strong warming effect associated with reduced evapotranspiration. However, forest removal in the temperate and high-latitude regions cools surface climate because the dominant mechanism is albedo increase that leads to lower shortwave radiation absorption in the cleared land (Bounoua et al., 2002; Snyder et al., 2004). This cooling effect is particularly strong in the boreal regions where the snow mask effect amplifies the albedo induced cooling (Bonan et al., 1992, 1995). In agreement with the climate model experiments, empirical studies using in-situ air temperature (Lee et al., 2011; Zhang et al., 2014) and satellite-derived land surface temperature (Li et al., 2015) also show that the temperature effects of forests have a clear latitudinal pattern.

Albedo and evapotranspiration are the two major biophysical mechanisms through which deforestation affects temperature and thereby causes the latitudinal pattern (Gibbard et al., 2005). However, due to high spatial variability of biophysical properties, it is still unclear, at a particular location, which mechanism dominates and what the net effect would be if forest is removed. This is further complicated by the influence of the background climate on the altered water and energy balance. Previous studies show that climate conditions such as snow and rainfall play an important role because biophysical effects can be either enhanced or dampened under different climate regimes,

ESDD
6, 1897–1937, 2015

making temperature change more spatially variable (Pitman et al., 2011; Li et al., 2015). Such complexity is reflected in the temperate forests where the two biophysical mechanisms with opposite effects tend to cancel each other, making their net effect much more uncertain compared to other forests. This was shown clearly by the mixed results obtained from modeling and observational studies (Bonan, 2008; Wickham et al., 2013; Li et al., 2015). Furthermore, changes in the other energy components such as sensible heat and multiple atmospheric feedbacks that are triggered by deforestation can in turn modify the albedo and evapotranspiration impact. Therefore, it is important to further investigate the relative strength of the impact of albedo and evapotranspiration on temperature change, and how much they are influenced by the interaction with the local climate and other factors.

The spatial scale of deforestation is also important for its climatic impact. It has been shown that deforestation impact is sensitive to spatial extent (global-regional-local) and degree of vegetation change, from partial disturbance to complete removal (Sampaio et al., 2007; Longobardi et al., 2012). For example, there is evidence that in the Amazon area, precipitation change can exhibit either a linear or non-linear relationship with vegetation change, depending on the spatial scale of deforestation, and could be opposite in sign (Avissar et al., 2002; Baidya Roy and Avissar, 2002; Souza and Oyama, 2010; Runyan, 2012). It is still not clear whether the temperature has such scale-dependent behavior, and whether the latitudinal pattern of temperature response would be modified.

Deforestation impact originates from the altered biophysical properties such as albedo, roughness, canopy conductance, surface emissivity, etc., which cause temperature change via different paths. Some of these factors may have inherent latitudinal patterns. For instance, the albedo difference between forest and open land increases with latitude (Li et al., 2015). The question now would be whether the latitudinal temperature response to deforestation can be attributed to biophysical changes, per se, or to the processes that translate perturbations to surface climate response, or to both. The answer to this question requires knowing how individual biophysical changes contribute to temperature change. Efforts have been made to quantify the contribution of each biophysical factor, including both empirical (Juang et al., 2007) and modeling studies (Lean and Rowntree, 1997; Maynard and Royer, 2004; Davin and de Noblet-Ducoudre, 2010) that enable us to decompose the temperature change into components. Such studies can improve our knowledge of the mechanisms for the climate impact induced by vegetation change.

In this study, we use an earth system model to investigate how deforestation affects temperature via biophysical changes and to examine which physical mechanisms are responsible for the latitude-dependent temperature response (Sect. 2). We first analyze latitudinal temperature changes in response to multiple deforestation scenarios and their scale-dependence (Sects. 3.1 and 3.2), and then explore the possible causes for the latitudinal and spatial pattern from the surface energy balance (Sect. 3.3) as well as the role of background climate (Sect. 3.4). Finally, we show how different biophysical mechanisms affect temperature change and discuss their contributions to the latitudinal pattern (Sect. 3.5). A brief discussion and summary are provided in Sect. 4.

2 Method

2.1 Model description

The UMD earth system model of intermediate complexity (Zeng, 2004) is used to perform the experiments. It consists of a global version of QTCM atmosphere model (Neelin and Zeng, 2000), a physical land surface model Sland (Zeng et al., 2000), a dynamic vegetation and carbon model VEGAS (Zeng, 2003; Zeng et al., 2005), and a slab ocean model but we use prescribed sea surface temperatures (SSTs) in our experiments.

Sland is a land surface model of intermediate complexity that is more complicated than the bucket model in its parameterization of evapotranspiration processes, aiming to model the first-order effects relevant to climate simulation. Vegetation parameters

ESDD
6, 1897–1937, 2015

such as leaf area index, roughness, stomatal conductance, and vegetation fraction depend on climate and are calculated by VEGAS. Surface albedo is the seasonal climatology obtained from satellite (Darnell et al., 1992). Vegetation-albedo feedback is treated in the model by introducing albedo anomalies, that is, adding the albedo change calculated by VEGAS onto the observed albedo climatology used by the atmospheric radiation module (Zeng and Yoon, 2009). It should be mentioned that Sland in its current setup does not explicitly account for surface snow, thus no snow-albedo feedback is included. This potentially leads to an underestimation of albedo change in regions with frequent snow, but it also offers a unique opportunity to examine the mechanisms other than snow in the temperature response to deforestation at high latitudes.

The dynamic vegetation model VEGAS is able to simulate the dynamics of vegetation growth and competition among different plant functional types (PFTs). Four plant functional types are included – broadleaf tree, needleleaf tree, cold grass, and warm grass – and their phenology is simulated dynamically as the balance between growth and respiration/turnover. The vegetation component is coupled to land and atmosphere through soil moisture dependence of photosynthesis and evapotranspiration, as well as dependence on temperature, radiation, and atmospheric CO_2. The earth system model is run at a resolution of $5.625^{\circ} \times 3.75^{\circ}$. The UMD earth system model has been used to study the climate and vegetation feedbacks (e.g., Zeng et al., 1999; Zeng and Neelin, 2000; Hales et al., 2004; Zeng and Yoon, 2009) and was part of the Coupled Climate–Carbon Cycle Model Intercomparison Project, C^4MIP (Friedlingstein et al., 2006).

2.2 Experiment design

UMD earth system model is a fully coupled model, but the setup for this study is an atmosphere–land-vegetation coupled version with prescribed ocean SST, and CO_2 concentration at the preindustrial level of 280 ppv. The model is driven by a climatological seasonal cycle of SST, averaged for 1960–1990 to smooth the influence of inter-annual climate variability. The model is first run for 500 years to allow for spin-up time during which vegetation is dynamically computed and reaches an equilibrium

Discussion Paper | Discussion Paper | Discussion Paper | Discussion Paper |
ESDD
6, 1897–1937, 2015
Spatial scale and background climate in the latitudinal temperature response
Y. Li et al.

state with climate. Figure S1 shows the potential vegetation map obtained by the end of model spin-up. The vegetation map generally has a reasonable geographical distribution but is not perfect, for example, vegetation in Sahara region. This is because vegetation is mainly determined by simulated climate in the model, thus any simulation bias in precipitation (Fig. S2) could influence the vegetation pattern more or less. For our analysis, the climatology over the last 10 years of spin-up is used as the control experiment (CTL). This is adequate for our simulation because of the small interannual variability in the model. Deforestation is imposed by setting the forest fraction in a given grid cell to zero (or a reduction with a given rate applied to the potential vegetation map), meaning forest is replaced by bare soil, as is also done in several previous studies (Bonan et al., 1992; Bounoua et al., 2002; Snyder, 2010). The sharp contrast between forest and bare ground is indicative of the maximum impact of deforestation. In the simulation for deforestation experiment, modified vegetation fractions are fixed so that the vegetation model becomes "static" rather than "dynamic".

Three groups of experiments are designed to study different aspects of the deforestation impact (Table 1): (I) deforestation with different spatial extents (II) with different deforestation fraction; (III) with individual biophysical factors changed separately. The first two groups address the spatial scale problem for the climatic response to deforestation. Group (I) consists of three regional deforestation scenarios that take place in the tropical (20° S–20° N), northern temperate (20–50° N) and boreal (50–90° N) regions, and one global deforestation scenario in which all forests are cleared. Group (II) consists of four global deforestation experiments in which forest fractions are reduced by varying degrees to its original coverage at 25 to 100 % (100 % clearing is the same to the global deforestation in group I, referred to ALL).

Group (III) is designed to separate the effect of individual biophysical factors by which deforestation affects climate. Inspired by Davin and de Noblet-Ducoudre (2010), three experiments are devised to quantify the impact from changes in albedo, roughness, and evapotranspiration efficiency. Our experiment for albedo and roughness differs from Davin and de Noblet-Ducoudre (2010), who compared the case with only "one

ESDD
6, 1897–1937, 2015

factor changed” with the case of “everything unchanged”. In contrast, we compared the case of “everything changed with one factor unchanged” with the case of “everything changed”. Therefore, our experiments are named as “noALB”, “noRGH”, and “EVA”. In noALB experiment, albedo change induced by forest removal is not passed to the atmosphere, which means “no albedo change” indeed in the atmosphere model as it reads observed albedo data, while other variables are still being affected by deforestation. Thus, the albedo effect can be isolated by calculating the difference (ALL – noALB) of noALB and regular global deforestation, ALL, which includes the albedo change. In noRGH experiment, roughness is set to be unaffected by forest clearing, therefore, the difference ALL – noRGH can be attributed to the roughness effect. The calculation of evapotranspiration involves many parameters. For example, both albedo and roughness can affect ET. Therefore, for EVA experiment, a different strategy is adopted by fixing both albedo and roughness (as in CTL) while other variables are allowed to change. Thus, the difference of EVA and control, EVA – CTL, reflects processes other than albedo and roughness that can affect ET, representing the pure hydrological effect of deforestation that refers to the ability of vegetation to transfer water from the soil to the atmosphere (Davin and de Noblet-Ducoudre, 2010).

All deforestation simulations are initialized with the restart files after spin-up whose vegetation map, relevant parameters, and model codes have been modified as described above. Each simulation is run for 100 years and the averaged results of the last 10 years are used for analysis. Ground temperature is used to analyze temperature change, because the model does not output the 2 m air temperature. Ground temperature has a strong signal of the locally induced temperature change, which is closely coupled to the surface energy balance. This enables us to focus on the local and regional impacts of vegetation change. Only model grid points with forest fractional change more than 0.1 are analyzed for robustness. The resulting changes in LAI, albedo, and roughness induced by global deforestation are provided in Supplement (Figs. S3–S5).

ESDD
6, 1897–1937, 2015

3 Results

3.1 Latitudinal temperature change to deforestation

The latitude-dependent temperature response is confirmed by the three regional deforestation experiments (see Fig. 1a–c for tropical, northern temperate and boreal, and Fig. 1d for global deforestation experiments). Because of small inter-annual variability, the deforestation impact shows a strong signal in the simulation and almost all changes over the land are of statistical significant, therefore significance levels are not shown on the map. In tropical deforestation (20° S–20° N) experiment, a significant and widespread warming is observed over deforested regions by 2.22 K (Table 2), greatest (~ 4 K) in the Amazon and Central Africa regions and about 1–2 K in South Asia and the east coast of Australia. Although warming is the dominant effect, there are areas around Sahel in which we observe cooling up to −2 K. This suggests temperature response can differ within a latitude band, as is shown in earlier studies (McGuffie et al., 1995; Snyder et al., 2004). The regional difference is partly due to the regional circulation patterns being affected differently by deforestation (McGuffie et al., 1995). Temperature outside the deforestation boundary (e.g., South Asia, North Canada) is also influenced by the tropical deforestation, indicating that the vegetation disturbance signal can spread to distant regions through atmospheric processes. Replacing forest with bare ground leads to a surface albedo increase of 0.26, and a decrease of shortwave absorption at the surface by 38 $\mathrm{W\,m^{-2}}$. Precipitation and evapotranspiration also decline drastically by 105 and 82 $\mathrm{W\,m^{-2}}$, respectively, while sensible heat increases. Reducing cloud cover results in an increase in downward shortwave and a decrease in downward longwave radiation (Table 2).

In the northern temperate region (20–50° N), deforestation causes a temperature decrease of −0.84 K over most areas. North China and most parts of the United States show the largest cooling (~ −1.5 K) while a weaker cooling (< −1 K) is observed in Europe. Nevertheless, temperature rise can be found in some areas like South China (1 ~ 2 K) and Southeast US (~ 1 K), similar to the tropics. The regional difference also

ESDD
6, 1897–1937, 2015

reflects the different response of the surface energy balance to deforestation, and is related to the background climate as discussed in the next section. Other changes, including increased albedo and decreased shortwave absorption as well as decrease in ET and precipitation, can be seen in temperate deforestation, but the magnitudes are much smaller than those in the tropics. Unlike the tropical region, sensible heat decreases in the temperate region and is consistent with the sign of temperature change.

Compared with the temperate region, deforestation in the boreal region results in a stronger cooling at −1.70 K but changes in the surface energy components are much smaller. It should be noted that albedo only increases by 0.21 because of no snow-masking effect in the land surface model, which could enhance the cooling signal by amplifying the albedo change. Nevertheless, a considerable cooling is seen in our results without the snow-masking effect, suggesting that other changes rather than snow contribute to the cooling effect of deforestation.

3.2 Sensitivity of temperature change to the spatial scale of deforestation

The influence of spatial extent of deforestation can be clearly seen by comparing the temperature response in a given region under regional and global deforestation experiments. While similar in spatial pattern, temperature change in the global deforestation experiment (Fig. 1d) is much stronger than those in the regional deforestation, especially in mid- and high-latitudes (Table 2). From the regional to global scale, deforestation-induced cooling increases from −0.84 to −1.56 K, and from −1.70 to −2.42 K in the northern temperate and boreal regions, respectively. In contrast, warming in the tropics is less affected and even slightly decreases from 2.22 K in the regional deforestation case to 2.06 K in the global case. This is because global deforestation leads to a stronger reduction of both absorbed shortwave radiation and downward longwave radiation, both amplifying the cooling effects (Table 2) that reduce tropical warming and enhance high-latitude cooling. Such dampened tropical warming and enhanced extra-tropical cooling from regional to global deforestation experiments are supported by a recent study (Devaraju et al., 2015). Overall, an amplified temperature change in

ESDD
6, 1897–1937, 2015

the global deforestation experiment is expected as it generates a stronger perturbation to the atmosphere, but the latitudinal temperature response is well preserved despite different spatial scales.

Beside the spatial extent of deforestation, temperature change is also sensitive to deforestation fraction, the percentage of trees removed relative to the original coverage, which is equivalent to real areas that have been deforested (25, 50, 75 %, and 100 %, see Fig. 2 and Table 3). For 25 % deforestation fraction, temperature is virtually unaffected in most areas except for a weak warming in the tropics. As forest loss fraction goes up to 50 %, a latitudinal temperature change emerges with discernible tropical warming and weak cooling in mid- and high-latitudes (Fig. 3). Higher deforestation fractions of 75 and 100 % result in a greater temperature change and a more prominent latitudinal pattern. Generally, the magnitude of temperature change responds to increasing deforestation fractions nonlinearly with much larger changes at high deforestation fractions (Fig. 3, Table 3). This nonlinearity arises because the induced biophysical change as a perturbation (e.g., albedo change) does not increase linearly with deforestation fraction, while temperature change and biophysical change show linearly.

3.3 Role of surface energy balance in latitudinal temperature change

Temperature change is driven by altered surface energy balance in response to forest removal. Among them, changes in shortwave radiation absorption (ΔSW) and evapotranspiration (ΔET) can largely determine the sign and magnitude of temperature response to deforestation. Deforestation can increase surface albedo, leading to reduced absorbed shortwave radiation at the surface (ΔSW) which acts as a cooling mechanism, while decreased ET (ΔET) can produce a warming effect due to weakened latent cooling.

Figure 4c shows the latitudinal pattern of ΔSW and ΔET. Although the largest decreases are observed in the low latitudes and become smaller as latitude increases, the relative importance of these two varies across latitudes as also reported in Davin and de Noblet-Ducoudre (2010) and Li et al. (2015). In the tropics, ET declines (warming ef-

ESDD
6, 1897–1937, 2015

fect) more than the absorbed shortwave radiation (cooling effect). This ΔET-dominated energy imbalance is compensated by increase in temperature, outgoing longwave radiation, and sensible heat. Beyond the tropics, the opposite occurs, as ET declines less than absorbed shortwave radiation, therefore temperature and sensible heat decrease in response to the ΔSW dominated energy imbalance. Specifically, mid-latitude is a transition region where ΔET and ΔSW in the south are relatively close to each other but in the north are quite different. In high latitudes, ΔET is negligible whereas ΔSW maintains similar magnitude as in the mid latitudes, thus resulting in the most significant temperature decrease.

Although ΔSW and ΔET determine the basic latitudinal pattern of temperature change, changes in downward longwave radiation (ΔLW↓) and sensible heat (ΔH) also have influence. While ΔSW↓ (changes in downward shortwave) could be considered as a part of atmospheric feedback due to cloud cover change, we find that ΔSW is still dominated by ΔSW↑ (changes in upward shortwave) due to albedo change (Fig. S6). ΔLW↓ decreases across all latitudes due to less cloud cover, while sensible heat increases in the tropics and decreases in other latitudes. ΔLW↓ is combined with ΔSW to give the available energy ($\Delta \text{Ava} = \Delta \text{SW} + \Delta \text{LW}\downarrow$) and ΔH is combined with ΔET to give the turbulence energy ($\Delta \text{Tub} = \Delta \text{ET} + \Delta \text{H}$), corresponding to the changes in received and dissipated energy, respectively. More available energy warms the land surface while more turbulence energy cools the surface (de Noblet-Ducoudré et al., 2012). The difference of these two is the outgoing longwave radiation, which is a function of ground temperature and is equivalent to ground temperature change. As shown in Fig. 4d, the latitudinal changes of the available and turbulence energy largely resemble that of ΔSW and ΔET, but with some noticeable differences. Comparing with ΔSW, reduction in available energy (ΔAva) is larger across all latitudes, suggesting an amplifying feedback mechanism through ΔLW↓ due to reduced cloud cover (more reduction in $\Delta \text{SW} + \Delta \text{LW}\downarrow$, Fig. 4a). However, ΔTub is smaller than ΔET in the tropics (less reduction for $\Delta \text{ET} + \Delta \text{H}$, Fig. 4b) but larger than ΔET in the mid and high latitudes (more reduction for $\Delta \text{ET} + \Delta \text{H}$, Fig. 4b), showing that the warming signal can be

ESDD
6, 1897–1937, 2015

Spatial scale and background climate in the latitudinal temperature response

Y. Li et al.

Title Page
Abstract Introduction
Conclusions References
Tables Figures
Back Close
Full Screen / Esc
Printer-friendly Version
Interactive Discussion

either weakened or enhanced when ΔH is considered. Overall, the latitude pattern of ΔSW and ΔET in the Southern Hemisphere is influenced more by $\Delta LW\downarrow$ and ΔH than in the Northern Hemisphere. In the Southern Hemisphere, the originally large energy difference between ΔSW and ΔET disappears when $\Delta LW\downarrow$ and ΔH are accounted for, resulting in a dampened energy difference of ΔAve and ΔTub.

Analysis above shows that the basic latitudinal pattern of ΔSW and ΔET can explain most of the latitudinal temperature response regardless of other changes and feedbacks (e.g., changes in downward longwave and sensible heat). Here we evaluate the extent to which relative importance of ΔSW and ΔET can explain the spatially varying temperature change in terms of its sign and amplitude. The sign of temperature change can be approximated by a simple ratio of $\Delta ET/\Delta SW$. The accuracy of this approximation depends on the strength of the basic pattern imposed by ΔSW and ΔET against other changes. A larger-than-one ratio suggests ΔET warming exceeds ΔSW cooling and temperature is likely to increase. On the contrary, a smaller-than-one ratio suggests ΔSW cooling is stronger than ΔET warming and temperature tends to decrease. We used data from regional deforestation experiments to demonstrate this feature. Fig. 5 shows the deforested grid points in the model with their ΔET and ΔSW plotted on the x and y axes, with colors representing the sign of temperature change. Deforested points with increased temperature (red) are often located in the upper-left space of the $\Delta ET = \Delta SW$ line where warming is anticipated ($\Delta ET > \Delta SW$), while points with decreased temperature fall into the lower-right space where cooling is anticipated ($\Delta ET < \Delta SW$). It turns out that ΔET and ΔSW alone can explain 93, 88, and 99 % of deforested points for the direction of temperature change in the tropical, temperate, and boreal regions, respectively. In addition, there is tendency towards larger ratios at higher latitudes and wetter areas in the global deforestation experiment (Fig. S7), suggesting a decreasing importance of ΔET over ΔSW. A few exceptions exist because longwave and sensible heat changes may also influence temperature change but are not considered here. Furthermore, the amplitude of temperature change is related to the difference of ΔSW and ΔET. As shown in Fig. 5d–f, $\Delta SW - \Delta ET$ is highly correlated with the amplitude of temperature change in the tropical ($r = 0.96$) and temperate regions ($r = 0.79$), but not in the boreal region ($r = 0.27$).

3.4 Influence of background climate on surface energy change

The latitude-dependent pattern for ΔSW and ΔET could arise from the intrinsic latitudinal distribution in background climate, e.g., solar radiation and precipitation/ET decrease with latitude increase. Therefore, the same amount of albedo change would translate into a larger ΔSW in lower latitudes due to the geographic distribution of solar radiation. Likewise, given the same ET reduction rate, a larger ΔET is expected in the tropics than in high latitudes.

The influence of background climate can be illustrated by a simple calculation. Assume that deforestation causes albedo increase by 0.02, 0.05, 0.12, and 0.23 uniformly across all latitudes and ET decrease by 15, 30, 50, and 75 % compared to their baseline climatology, respectively. Multiplying these change rates by the baseline shortwave radiation and ET, we obtain the corresponding ΔSW and ΔET without considering any climate feedback. For demonstration purpose, the change rates chosen here for albedo and ET are somewhat arbitrary, roughly corresponding to the global averaged change in the four deforestation fraction experiments (deforestation fraction ranges from 25 to 100 %, see group II experiment). Interestingly, the calculated ΔSW and ΔET (Fig. 6) agree well with the simulation (Fig. 4c). The main features, including ΔET > ΔSW in the tropics and ΔET < ΔSW in the extratropics, are captured. We also used the satellite derived ET and shortwave radiation data from Li et al. (2015) to perform the calculation (see Fig. S8). The results generally support the findings from Fig. 6, except two combinations with small changes in albedo and ET. For these two cases, the anticipated pattern is not captured mainly because the chosen low albedo change in high latitude, which leads to an underestimation of ΔSW. It should be emphasized that the albedo and ET change rates in reality have more complicated patterns than what we assume in the calculation. Nevertheless, our simple calculation still reveals the role of the baseline climate in shaping the latitude-dependent temperature change to deforestation.

ESDD
6, 1897–1937, 2015

Further evidence comes from the spatial relationship between background climate and temperature response to deforestation. We found baseline precipitation is highly correlated with ΔET ($r = -0.98$) and with ΔT ($r = 0.87$), suggesting that precipitation can influence temperature change by controlling ET change. This is also supported by the ratio of ΔET/ΔSW in Fig. S7 where larger ΔET over ΔSW is found in wetter areas, and by observations from air temperature (Zhang et al., 2014) and physical mechanisms pertaining to soil moisture (Swann et al., 2012). Therefore, spatial variation of temperature change is partly due to background climate. For instance, temperature decreases in the tropical deforested areas like Sahel, west Amazon, and southwestern Africa because dry climate limits ΔET, thus temperature change is dominated by the cooling effect from ΔSW. In contrast, in wet temperate deforested areas like South China, India, and parts of North America, temperature increases because of the dominant warming effect from ΔET.

3.5 Contribution of individual biophysical processes to the latitudinal temperature change

The aforementioned changes in temperature and surface energy balance are triggered due to the altered biophysical variables such as albedo, roughness, ET efficiency, etc. as a result of deforestation. The effect of each individual biophysical factor and its contribution to temperature change are evaluated in this section.

3.5.1 Albedo

The impact of albedo change can be isolated by the difference of ALL – noALB (see Sect. 2), as shown in Fig. 7a. As expected, albedo change causes significant temperature decrease over all affected regions. Surprisingly, the strongest cooling appears in the northern temperate region instead of the tropics where the largest albedo increase occurs (Table 4). This indicates the strength of perturbation is not the only factor for determining spatially varying temperature change. The magnitude of cooling in the boreal

ESDD
6, 1897–1937, 2015

region is similar to the temperate region, because of no amplified albedo change due to snow. If deforestation does not change albedo, there would be a substantial warming over all affected regions (noALB – CTL, Fig. 7b), accompanied with decreased ET and very little change in absorbed shortwave radiation (SW). This is expected because the warming effect of ΔET dominates temperature change when albedo effect is absent.

3.5.2 Roughness

Roughness can affect turbulence (ET as well as sensible heat) flux between land surface and atmosphere. Higher roughness facilitates absorbed shortwave energy to be dissipated as turbulence, while smaller roughness suppresses this process and could have a warming effect. Roughness change is more pronounced in the tropical region (Table 4) where its effect on climate can be isolated by considering the difference All – noRGH. As is seen in Fig. 8a, reduced roughness warms most areas except for the upper northern latitudes, with warming decreasing from the tropics to high latitudes; see also Davin and de Noblet-Ducoudre (2010). Without roughness change, deforestation would cause less warming (Fig. 8b) and less reduction in turbulence energy (not shown) than regular deforestation. Presence of tropical warming in some areas in Fig. 8b implies that the reduction in evapotranspiration efficiency remains dominant and outweighs the albedo impact despite the change in roughness.

3.5.3 Evapotranspiration efficiency

Evapotranspiration efficiency refers to the ability of partitioning available energy into evapotranspiration more than into sensible heat. The conversion of forest to bare land favors more turbulence energy to be transferred in the form of sensible heat rather than ET, resulting in lower ET and higher sensible heat. The impact of altered ET efficiency can be separated by EVA – CTL, showing a noticeable warming in the tropical regions and some parts of the temperate region, and negligible impact in high latitude (Fig. 9).

ESDD
6, 1897–1937, 2015

It seems that changed ET efficiency has a significant impact only over regions with wet climate, which may be due to the close coupling between precipitation and ET change.

By summing up the contributions from individual biophysical factors linearly (ALL – noALB + ALL – noRGH + EVA – CTL), we reconstruct temperature change, which closely agrees with the actual signal (ALL – CTL) in terms of both latitudinal (Fig. 10) and geographical patterns (Fig. 11). Latitudinal features are inherited in the contribution of each individual component (Table 4). Albedo effect generally increases with latitude whereas roughness and evapotranspiration efficiency effects decrease with latitude. Therefore, the largest temperature increase in the tropical region (2.06 K) originates from the warming effect of changed roughness (1.92 K) and evapotranspiration efficiency (1.22 K), and is counteracted by a comparatively small albedo cooling (−1.92 K). In the extratropics, temperature response is dominated by albedo cooling, with similar strengths in the northern temperate (−3.01 K) and boreal (−2.93 K) regions. But such cooling is partially canceled by the weaker warming effect of roughness (0.86 K) and evapotranspiration efficiency (0.27 K) in the temperate region and no compensation at all in the boreal region. The latitudinal pattern caused by each biophysical factor is less likely to be due to the latitudinal signal from biophysical change per se, because biophysical change does not match the latitude pattern of temperature response. For example, the largest temperature change does not occur where the largest biophysical change (e.g., albedo and roughness) occurs. This shows the complex interactions in the translation from the initial perturbation to subsequent climate response, which varies by latitude. Biophysical impacts are perhaps strongly regulated by the baseline climate where vegetation change occurs, as also demonstrated in Pitman et al. (2011).

4 Discussion

The patterns, shown in our results, of temperature change as a result of deforestation are in line with the conclusions of the previous modeling studies, e.g., strong tropical

ESDD
6, 1897–1937, 2015

warming (Nobre et al., 1991; Snyder et al., 2004), moderate temperate cooling, and strong boreal cooling (Bonan et al., 1992, 1995; Betts, 2000), but very few of them considers the spatial scale of deforestation. We found that temperature change varies nonlinearly with both the spatial scale and the fraction of forest removed, with increasingly larger temperature change as disturbance grows and little change in the latitudinal pattern. This scale-dependent feature in temperature change reflects a perturbation-response relationship derived from the existing mechanisms of the model, but it does not exactly emulate the influence of physical processes operating at various scales in the real world, because many scale-related processes cannot be fully resolved in a model with a given complexity. For example, many meso-scale processes cannot be included in a global model. This makes it difficult to compare our results to those from observational studies that span different spatial scales.

We found that changes in shortwave radiation absorption (ΔSW) and evapotranspiration (ΔET) can largely determine the sign and amplitude of temperature change and its latitudinal and spatial patterns in response to deforestation. Globally, among those deforested points, more than 90 % of the sign of temperature change can be explained by ΔSW and ΔET. Although ΔET and ΔSW can be influenced by other factors and feedbacks, they still provide useful diagnostic information for temperature change and serve as a first order approximation. Therefore, albedo and ET changes can be potentially applied to evaluate the possible impact of undergoing land cover change on local and regional temperature (Loarie et al., 2011; Peng et al., 2014; Li et al., 2015) as these two variables are readily available from satellite data.

The latitude-dependent temperature response to deforestation and its spatial variability, to a large extent, can be attributed to background climate condition, such as solar radiation, precipitation, and snow, which in turn affect biophysical impact of vegetation change. Further evidence comes from the contribution of each biophysical factor, i.e., albedo, roughness, and ET efficiency, on the temperature response. Although these factors drive temperature change into different directions, the latitudinal patterns of their contributions are similar (Davin and de Noblet-Ducoudre, 2010). This indicates

ESDD
6, 1897–1937, 2015

that the influence of climate condition manifests itself either explicitly in the temperature response through controlling changes on surface energy balance, or implicitly in the perturbation triggered by deforestation because biophysical characteristic itself is a result of complex interplay of vegetation and climate condition. Nevertheless, our results show that the former explains the latitudinal pattern.

We acknowledge certain limitations and important issues that have not been fully addressed in this study. Previous studies showed an important role of oceanic feedback which could cause additional cooling through albedo change (e.g., sea-ice albedo feedback) and could override temperature change over land in mid latitudes (Claussen et al., 2001; Davin and de Noblet-Ducoudre, 2010), but our ocean model is not interactive so such dynamics could not be studied here. Another question is the temperature variable used for studying the deforestation impact. Ground temperature instead of air temperature is analyzed here due to our model structure. Although air temperature is more widely used in the climate science community, research based on ground temperature (McGuffie et al., 1995; Kendra Gotangco Castillo and Gurney, 2012) or surface temperature (Davin and de Noblet-Ducoudre, 2010) is also seen in the literature. Despite the fact that some studies have shown that ground temperature (skin temperature) is in good agreement with air temperature at larger scales (Jin et al., 1997), it is worth investigating to what extent the results of ground temperature can resemble that of surface air temperature, since there is growing evidence suggesting that these two variables could have very different responses to vegetation change (Baldocchi and Ma, 2013; Zhao and Jackson, 2014; Li et al., 2015). Moreover, the response of maximum and minimum temperatures also differ from the daily averaged temperature (Zhang et al., 2014; Li et al., 2015), a problem that has received less attention in modeling studies. Further, results from a single model are subject to uncertainty and some features might be model-dependent. For instance, some biases in the simulated climate of the model may lead to shifts in vegetation distribution and thus could influence the deforestation impact. Therefore, model inter-comparison projects like Land-Use and Climate, Identification of Robust Impacts (LUCID) experiments (Pitman et al.,

ESDD
6, 1897–1937, 2015

2009) can help to distinguish robust findings against model uncertainty. The participant models in LUCID show consistency in how land cover change affects available energy but diverge greatly on energy partition between latent and sensible heat flux changes (de Noblet-Ducoudré et al., 2012), indicating large uncertainty lies in the response of non-radiative process to land cover change, especially for ET (Boisier et al., 2012). Therefore, considerable efforts are required to improve model performance in the simulation of land process and new inter-comparison projects such as LUMIP (Land Use Model Intercomparison Project) are highly desirable. In addition, observational studies are indispensable as they can offer new insights and serve as a reference benchmark for model results, especially those using new techniques and datasets such as satellite data.

The Supplement related to this article is available online at doi:10.5194/esdd-6-1897-2015-supplement.

Author contributions. Y. Li designed and carried out the experiments; Y. Li and N. de Noblet-Ducoudré analyzed the data; all authors contributed to the discussion and writing of the paper.

Acknowledgement. This work is supported by the National Natural Science Foundation of China (Nos. 41130534 and 41371096). Y. Li is supported by the China Scholar Council fellowship (No. 201306010169). We thank Andy Pitman for his constrictive and insightful comments to this paper. Y. Li thanks Fang Zhao for helps on running the model.

References

Allen, C. D., Macalady, A. K., Chenchouni, H., Bachelet, D., McDowell, N., Vennetier, M., Kitzberger, T., Rigling, A., Breshears, D. D., Hogg, E. H., Gonzalez, P., Fensham, R., Zhang, Z., Castro, J., Demidova, N., Lim, J. H., Allard, G., Running, S. W., Semerci, A., and Cobb, N.: A global overview of drought and heat-induced tree mortality reveals emerging climate change risks for forests, Forest Ecol. Manag., 259, 660–684, 2010.

ESDD
6, 1897–1937, 2015

Avissar, R., Silva Dias, P. L., Sivla Dias, M. A. F., and Nobre, C.: The large-scale biosphere–atmosphere experiment in Amazonia (LBA): insights and future research needs, J. Geophys. Res., 107, 1–6, 2002.
Baidya Roy, S. and Avissar, R.: Impact of land use/land cover change on regional hydrometeorology in Amazonia. J. Geophys. Res., 107, 8037, doi:10.1029/2000JD000266, 2002.
Baldocchi, D. and Ma, S.: How will land use affect air temperature in the surface boundary layer? Lessons learned from a comparative study on the energy balance of an oak savanna and annual grassland, Tellus B, 1, 1–19, 2013.
Betts, R. A.: Offset of the potential carbon sink from boreal forestation by decreases in surface albedo, Nature, 408, 187–190, 2000.
Betts, R. A., Falloon, P. D., Goldewijk, K. K., and Ramankutty, N.: Biogeophysical effects of land use on climate: model simulations of radiative forcing and large-scale temperature change, Agr. Forest Meteorol., 142, 216–233, 2007.
Boisier, J. P., de Noblet-Ducoudré, N., Pitman, A. J., Cruz, F. T., Delire, C., van den Hurk, B. J. J. M., van der Molen, M. K., Müller, C., and Voldoire, A.: Attributing the impacts of land-cover changes in temperate regions on surface temperature and heat fluxes to specific causes: results from the first LUCID set of simulations, J. Geophys. Res.-Atmos., 117, D12116, doi:10.1029/2011JD017106, 2012.
Bonan, G. B.: Forests and climate change: forcings, feedbacks, and the climate benefits of forests, Science, 320, 1444–1449, 2008.
Bonan, G. B., Pollard, D., and Thompson, S. L.: Effects of boreal forest vegetation on global climate, Nature, 359, 716–718, 1992.
Bonan, G. B., Chapin, F. S., and Thompson, S. L.: Boreal forest and tundra ecosystems as components of the climate system, Climatic Change, 29, 145–167, 1995.
Bounoua, L., DeFries, R., Collatz, G. J., Sellers, P., and Khan, H.: Effects of land cover conversion on surface climate, Clim. Change, 52, 29–64, 2002.
Claussen, M., Brovkin, V., and Ganopolski, A.: Biogeophysical versus biogeochemical feedbacks of large-scale land cover change, Geophys. Res. Lett., 28, 1011–1014, 2001.
Darnell, W. L., Staylor, W. F., Gupta, S. K., Ritchey, N. A., Wilber, A. C.: Seasonal variation of surface radiation budget derived from International Satellite Cloud Climatology Project C1 data, J. Geophys. Res.-Atmos., 97, 15741–15760, 1992.
Davin, E. L. and de Noblet-Ducoudre, N.: Climatic impact of global-scale deforestation: radiative versus nonradiative processes, J. Climate, 23, 97–112, 2010.

ESDD
6, 1897–1937, 2015

de Noblet-Ducoudré, N., Boisier, J. P., Pitman, A. J., Bonan, G. B., Brovkin, V., Cruz, F., Delire, C., Gayler, V., van den Hurk, B. J. J. M., Lawrence, P. J., van der Molen, M. K., Müller, C., Reick, C. H., Strengers, B. J., and Voldoire, A.: Determining robust impacts of land-use-induced land cover changes on surface climate over North America and Eurasia: results from the first set of LUCID experiments, J. Climate, 25, 3261–3281, 2012.
Devaraju, N., Bala, G., and Modak, A.: Effects of large-scale deforestation on precipitation in the monsoon regions: remote versus local effects, P. Natl. Acad. Sci. USA, 112, 3257–3236, 2015.
Friedlingstein, P., Cox, P., Betts, R., Bopp, L., von Bloh, W., Brovkin, V., Cadule, P., Doney, S. Eby, M., Fung, I., Bala, G., John, J., Jones, C., Joos, F., Kato, T., Kawamiya, M., Knorr, W., Lindsay, K., Matthews, H. D., Raddatz, T., Rayner, P., Reick, C., Roeckner, E., Schnitzler, K. G., Schnur, R. Strassmann, K., Weaver, A. J., Yoshikawa, C., and Zeng, N.: Climate–carbon cycle feedback analysis: results from the C4MIP model intercomparison, J. Climate, 19, 3337–3353, 2006.
Gibbard, S., Caldeira, K., Bala, G., Phillips, T. J., and Wickett, M.: Climate effects of global land cover change, Geophys. Res. Lett., 32, L23705, doi:10.1029/2005GL024550, 2005.
Hales, K., Neelin, J. D., and Zeng, N.: Sensitivity of tropical land climate to leaf area index: role of surface conductance versus albedo, J. Climate, 17, 1459–1473, 2004.
Hansen, M., Potapov, P., and Moore, R.: High-resolution global maps of 21st-century forest cover change, Science, 850, 850–853, 2013.
Jin, M., Dickinson, R., and Vogelmann, A.: A comparison of CCM2-BATS skin temperature and surface–air temperature with satellite and surface observations, J. Climate, 10, 1505–1524, 1997.
Juang, J. Y., Katul, G., Siqueira, M., Stoy, P., and Novick, K.: Separating the effects of albedo from eco-physiological changes on surface temperature along a successional chronosequence in the southeastern United States, Geophys. Res. Lett., 34, L21408, doi:10.1029/2007GL031296, 2007.
Kendra Gotangco Castillo, C. and Gurney, K. R.: Exploring surface biophysical-climate sensitivity to tropical deforestation rates using a GCM: A feasibility study, Earth Interact., 16, 1–23, 2012.
Lean, J. and Rowntree, P.: Understanding the sensitivity of a GCM simulation of Amazonian deforestation to the specification of vegetation and soil characteristics, J. Climate, 10, 1216–1235, 1997.

ESDD
6, 1897–1937, 2015

Title Page
Abstract | Introduction
Conclusions | References
Tables | Figures
◀| |▶
◀ ▶
Back | Close
Full Screen / Esc
Printer-friendly Version
Interactive Discussion

Lee, X., Goulden, M. L., Hollinger, D. Y., Barr, A., Black, T. A., Bohrer, G., Bracho, R., Drake, B., Goldstein, A., Gu, L. H., Katul, G., Kolb, T., Law, B. E., Margolis, H., Meyers, T., Monson, R., Munger, W., Oren, R., Kyaw, T. P. U., Richardson, A. D., Schmid, H. P., Staebler, R., Wofsy, S., and Zhao, L.: Observed increase in local cooling effect of deforestation at higher latitudes, Nature, 479, 384–387, 2011.

Li, Y., Zhao, M., Motesharrei, S., Mu, Q., Kalnay, E., and Li, S.: Local cooling and warming effects of forest based on satellite data, Nature Comm., 6, 6603, doi:10.1038/ncomms7603, 2015.

Loarie, S. R., Lobell, D. B., Asner, G. P., Mu, Q., and Field, C. B.: Direct impacts on local climate of sugar-cane expansion in Brazil, Nature Clim. Change, 1, 105–109, 2011.

Longobardi, P., Montenegro, A., Beltrami, H., and Eby, M.: Spatial scale dependency of the modelled climatic response to deforestation, Biogeosciences Discuss., 9, 14639–14687, doi:10.5194/bgd-9-14639-2012, 2012.

Maynard, K. and Royer, J.-F.: Sensitivity of a general circulation model to land surface parameters in African tropical deforestation experiments, Clim. Dynam., 22, 555–572, 2004.

McGuffie, K., Henderson-Sellers, A., Zhang, H., Durbidge, T. B., and Pitman, A. J.: Global climate sensitivity to tropical deforestation, Global Planet. Change, 10, 97–128, 1995.

Neelin, J. D. and Zeng, N.: A quasi-equilibrium tropical circulation model – formulation, J. Atmos. Sci., 57, 1741–1766, 2000.

Nobre, C., Sellers, P., and Shukla, J.: Amazonian deforestation and regional climate change, J. Climate, 4, 957–998, 1991.

Peng, S., Piao, S., Zeng, Z., Ciais, P., Zhou, L., Li, L. Z. X., Myneni, R. B., Yin, Y., and Zeng, H.: Afforestation in China cools local land surface temperature, P. Natl. Acad. Sci. USA, 111, 2915–2919, 2014.

Pitman, A. J., de Noblet-Ducoudré, N., Cruz, F. T., Davin, E. L., Bonan, G. B., Brovkin, V., Claussen, M., Delire, C., Ganzeveld, L., Gayler, V., van den Hurk, B. J. J. M., Lawrence, P. J., van der Molen, M. K., Müller, C., Reick, C. H., Seneviratne, S. I., Strengers, B. J., and Voldoire, A.: Uncertainties in climate responses to past land cover change: first results from the LUCID intercomparison study, Geophys. Res. Lett., 36, L14814, doi:10.1029/2009GL039076, 2009.

Pitman, A. J., Avila, F. B., Abramowitz, G., Wang, Y. P., Phipps, S. J., and de Noblet-Ducoudre, N.: Importance of background climate in determining impact of land-cover change on regional climate, Nature Clim. Change, 1, 472–475, 2011.

Pitman, A. J., Arneth, A., and Ganzeveld, L.: Regionalizing global climate models, Int. J. Climatol., 32, 321–337, 2012.
Runyan, C.: Physical and biological feedbacks of deforestation, Rev. Geophys., 50, 1–32, 2012.
Sampaio, G., Nobre, C., Costa, M. H., Satyamurty, P., Soares-Filho, B. S., and Cardoso, M.: Regional climate change over eastern Amazonia caused by pasture and soybean cropland expansion, Geophys. Res. Lett., 34, L17709, doi:10.1029/2007GL030612, 2007.
Snyder, P. K.: The influence of tropical deforestation on the Northern Hemisphere climate by atmospheric teleconnections, Earth Interact., 14, 1–34, 2010.
Snyder, P. K., Delire, C., and Foley, J. A.: Evaluating the influence of different vegetation biomes on the global climate, Clim. Dynam., 23, 279–302, 2004.
Souza, D. C. and Oyama, M. D.: Climatic consequences of gradual desertification in the semi-arid area of Northeast Brazil, Theor. Appl. Climatol., 103, 345–357, 2010.
Swann, A. L. S., Fung, I. Y., and Chiang, J. C. H.: Mid-latitude afforestation shifts general circulation and tropical precipitation, P. Natl. Acad. Sci. USA, 109, 712–716, 2012.
Wickham, J. D., Wade, T. G., and Riitters, K. H.: Empirical analysis of the influence of forest extent on annual and seasonal surface temperatures for the continental United States, edited by: Peñuelas, J., Global Ecol. Biogeogr., 22, 620–629, 2013.
Zeng, N.: Glacial–interglacial atmospheric CO_2 change – the glacial burial hypothesis, Adv. Atmos. Sci., 20, 677–693, 2003.
Zeng, N.: How strong is carbon cycle-climate feedback under global warming?, Geophys. Res. Lett., 31, L20203, doi:10.1029/2004GL020904, 2004.
Zeng, N. and Neelin, J. D.: The role of vegetation climate interaction and interannual variability in shaping the African Savanna, J. Climate, 13, 2665–2670, 2000.
Zeng, N. and Yoon, J.: Expansion of the world's deserts due to vegetation-albedo feedback under global warming, Geophys. Res. Lett., 36, L17401, doi:10.1029/2009GL039699, 2009.
Zeng, N., Neelin, J. D., Lau, K. M., and Tucker, C. J.: Enhancement of interdecadal climate variability in the Sahel by vegetation interaction, Science, 286, 1537–1540, 1999.
Zeng, N., Neelin, J. D., and Chou, C.: A quasi-equilibrium tropical circulation model – implementation and simulation, J. Atmos. Sci., 57, 1767–1796, 2000.
Zeng, N., Mariotti, A., and Wetzel, P.: Terrestrial mechanisms of interannual CO_2 variability, Global Biogeochem. Cy., 19, 1–15, 2005.
Zhang, M., Lee, X., Yu, G., Han, S., Wang, H., Yan, J., Zhang, Y., Li, Y., Ohta, T., Hirano, T., Kim, J., Yoshifuji, N., and Wang, W.: Response of surface air temperature to small-scale land

ESDD
6, 1897–1937, 2015

clearing across latitudes, Environ. Res. Lett., 9, 034002, doi:10.1088/1748-9326/9/3/034002, 2014.
Zhao, K. and Jackson, R.: Biophysical forcings of land-use changes from potential forestry activities in North America, Ecol. Monogr., 84, 329–353, 2014.

ESDD
6, 1897–1937, 2015

Spatial scale and background climate in the latitudinal temperature response

Y. Li et al.

Table 1. Deforestation experiment design.

Group	I. Spatial extent	II. Deforestation fractions	III. Biophysical factors
Experiment	Tropical Temperate Boreal Global	25 % forest removal 50 % forest removal 75 % forest removal 100 % forest removal	Albedo Roughness Evapotranspiration efficiency

ESDD
6, 1897–1937, 2015

Table 2. Annual mean changes in key climate variables in regional and global deforestation experiments relative to the control experiment. ΔSW is short for net shortwave change; the symbol "↑" denotes upward and "↓" denotes downward. Units are $W\,m^{-2}$ except for temperature (K) and albedo (%).

	Tropical (20° N–20° S)		Temperate (20–50° N)		Boreal (50–90° N)	
	Regional	Global	Regional	Global	Regional	Global
Δ Temperature	2.22	2.06	−0.84	−1.56	−1.70	−2.42
Δ Precipitation	−105	−109	−20	−25	−4	−6
ΔET	−82	−85	−17	−21	−5	−5
Δ Sensible heat	15	13	−12	−13	−14	−14
Δ Shortwave ↓	50	53	18	21	13	14
Δ Shortwave ↑	88	95	41	48	37	38
ΔLW↓	−14	−17	−11	−17	−6	−11
ΔSW	−38	−42	−23	−27	−24	−24
Δ Albedo (%)	26	28	16	18	21	22
Δ Turbulent flux	−67	−72	−29	−34	−19	−19
Δ Available energy	−52	−59	−34	−44	−30	−35

ESDD
6, 1897–1937, 2015

Table 3. Annual mean changes in key climate variables in global deforestation with different deforestation fractions.

Region	Tropical (20° N–20° S)				Temperate (20–50° N)				Boreal (50–90° N)			
Deforestation rate	25 %	50 %	75 %	100 %	25 %	50 %	75 %	100 %	25 %	50 %	75 %	100 %
ΔTemperature	0.53	1.22	1.86	2.06	0.03	−0.23	−0.75	−1.56	−0.17	−0.55	−1.21	−2.42
ΔPrecipitation	−16.1	−43.2	−73.5	−108.9	−4.8	−13.8	−20.0	−24.9	−0.7	−2.0	−3.3	−6.0
ΔET	−15.3	−37.1	−59.2	−85.5	−4.6	−12.4	−17.4	−20.7	−0.6	−1.6	−2.6	−5.2
ΔSensible heat	12.0	23.2	27.8	13.3	2.4	0.9	−4.1	−13.3	−1.2	−3.6	−8.0	−14.1
Δ Shortwave↓	3.8	13.1	27.1	52.6	1.7	7.7	14 0.1	21.3	1.4	3.9	7.7	13.8
Δ Shortwave↑	3.0	16.1	40.5	94.9	2.6	14.8	29.7	48.3	3.5	9.8	20.2	37.8
ΔLW↓	−0.7	−3.2	−6.7	−16.9	−1.2	−5.8	−10.6	−16.9	−0.8	−2.7	−5.6	−10.5
ΔAlbedo	0.87	4.7	12.1	27.7	1.0	5.6	11.1	18.0	2.2	6.1	12.2	21.9

All units are in $W\,m^{-2}$ except temperature (K) and albedo (%).

Discussion Paper | Discussion Paper | Discussion Paper | Discussion Paper |

ESDD

6, 1897–1937, 2015

Spatial scale and background climate in the latitudinal temperature response

Y. Li et al.

Table 4. Summary of influence of individual biophysical factors on temperature change (K).

	Global (ALL – CTL)	Albedo (ALL – noALB)	Roughness (ALL – noRGH)	Evapotranspiration efficiency (EVA – CTL)
50–90° N	−2.42	−2.93 (0.22)	0.05 (0.86)	0
20–50° N	−1.56	−3.1 (0.18)	0.86 (0.66)	0.27
20° S–20° N	2.06	−1.92 (0.28)	1.92 (1.33)	1.22

ALL: global deforestation; noALB: global deforestation without albedo change; noRGH: global deforestation without roughness change; EVA: global deforestation without both albedo and roughness change. Numbers in parentheses are changes in albedo and roughness.

ESDD
6, 1897–1937, 2015

Spatial scale and background climate in the latitudinal temperature response

Y. Li et al.

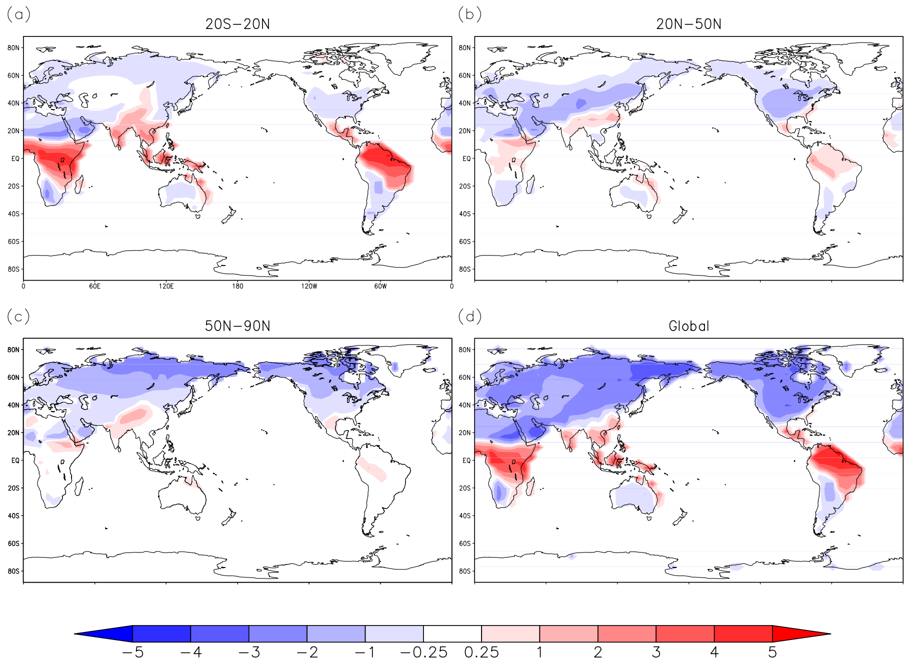

Figure 1. Ground temperature change for **(a)** tropical (20° S–20° N), **(b)** northern temperate (20–50° N), **(c)** boreal (50–90° N), and **(d)** global (90° S–90° N) deforestation (Unit: K).

ESDD
6, 1897–1937, 2015

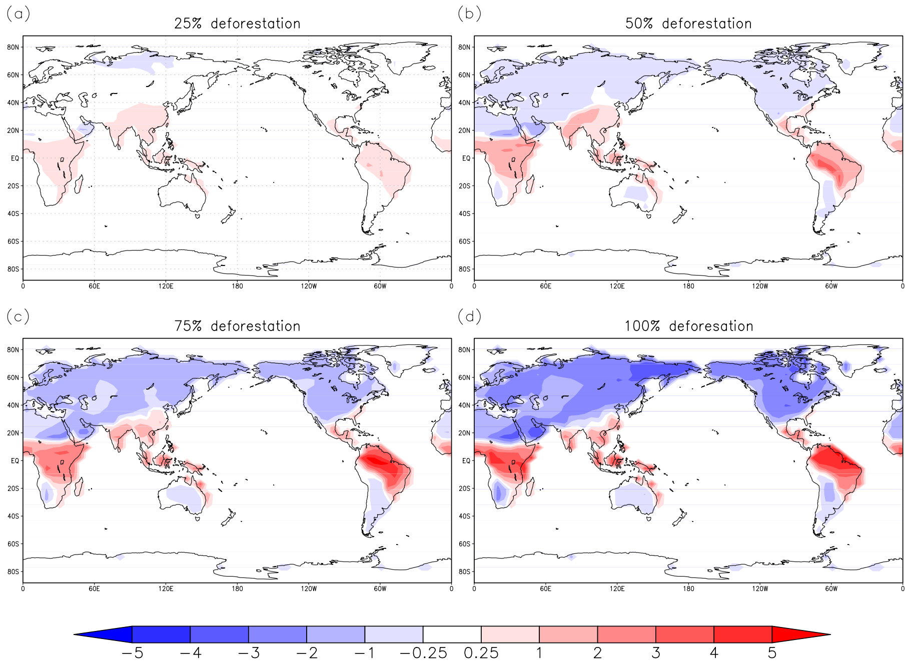

Figure 2. Temperature change for global deforestation experiments with different deforestation fractions at **(a)** 25 %, **(b)** 50 %, **(c)** 75 % and **(d)** 100 %.

ESDD
6, 1897–1937, 2015

Spatial scale and background climate in the latitudinal temperature response

Y. Li et al.

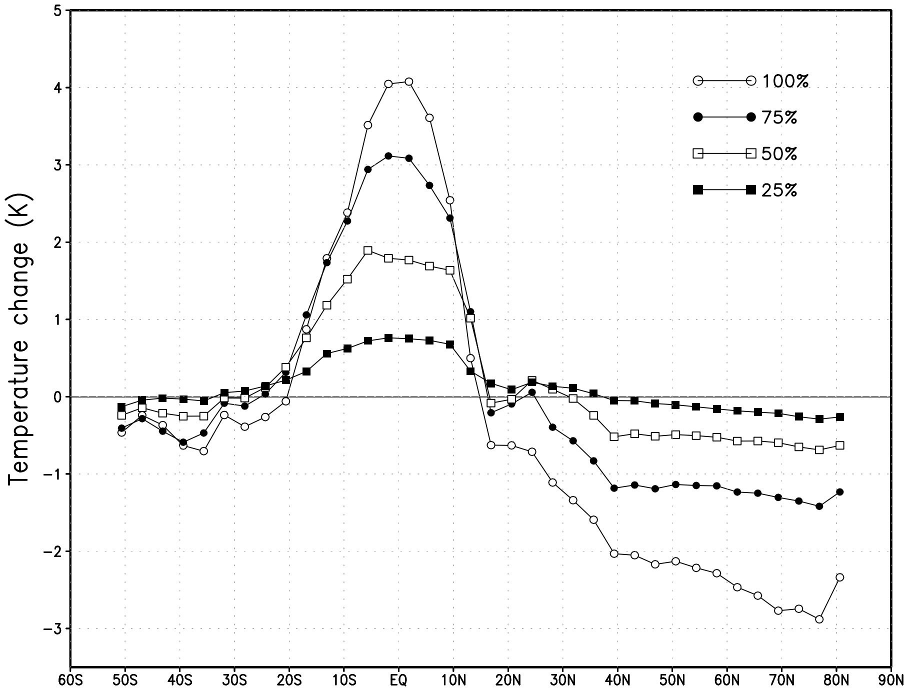

Figure 3. Latitudinal pattern of temperature change with different deforestation fractions (averaged over deforested areas).

ESDD
6, 1897–1937, 2015

Spatial scale and background climate in the latitudinal temperature response

Y. Li et al.

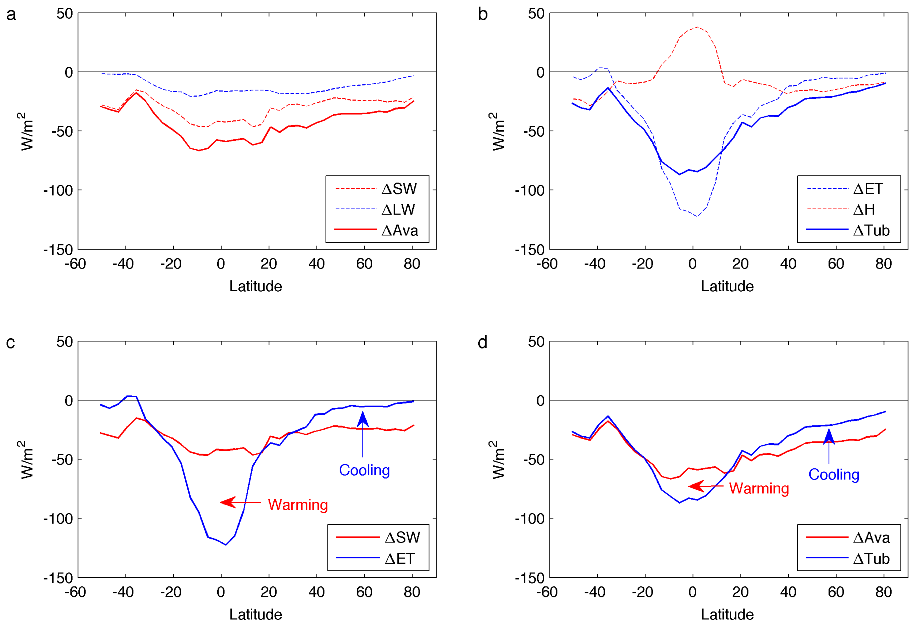

Figure 4. Latitudinal pattern of changes in surface energy balance. **(a)** Changes in absorbed shortwave radiation (ΔSW), downward longwave radiation (ΔLW↓), and available energy (ΔAva = ΔSW+ΔLW↓). **(b)** Changes in evapotranspiration (ΔET), sensible heat (ΔH), and turbulence energy (ΔTub = ΔET + ΔH). **(c)** ΔSW and ΔET. **(d)** ΔAva and ΔTub.

ESDD
6, 1897–1937, 2015

Spatial scale and background climate in the latitudinal temperature response

Y. Li et al.

Title Page
Abstract Introduction
Conclusions References
Tables Figures
Back Close
Full Screen / Esc
Printer-friendly Version
Interactive Discussion

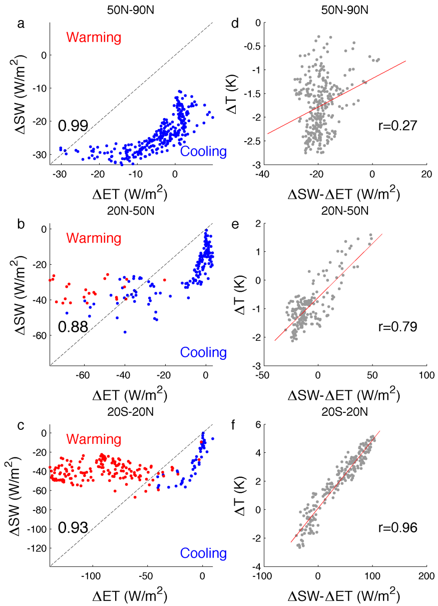

Figure 5. Changes in ET (ΔET), absorbed shortwave radiation (ΔSW) and their relationship with temperature change (ΔT) over deforestation areas. **(a–c)** Deforested points with their ΔSW, ΔET, and the sign of ΔT. The upper left area represents ET warming exceeds albedo cooling; the lower right area represents albedo cooling exceeds ET warming. Blue (red) are the actual grid points where temperature decreased (increased). Number denotes the percentage of deforested points whose sign of ΔT agrees with anticipation of ΔSW and ΔET. **(e, f)** Spatial relationship between ΔSW-ΔET and the amplitude of ΔT. Red line is the regression line, and r is the correlation coefficient. **(a, d)** Boreal deforestation. **(b, e)** Northern temperate deforestation **(c, f)** Tropical deforestation.

ESDD
6, 1897–1937, 2015

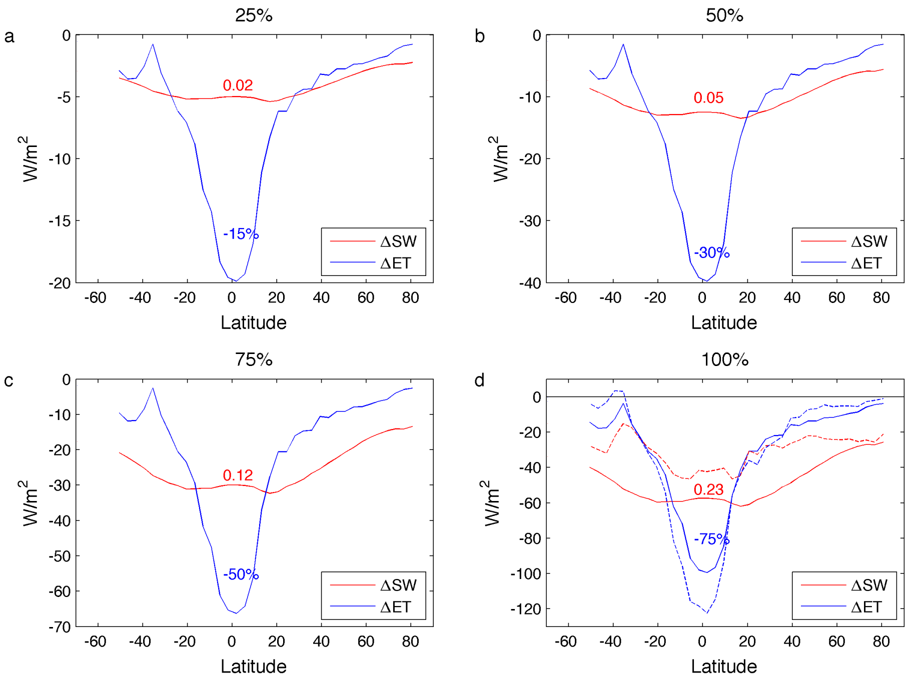

Figure 6. The latitudinal pattern of ΔSW and ΔET calculated by multiplying their background climate values with different rates for albedo (red number) and ET change (blue number). In **(d)**, dashed lines are simulated changes from global deforestation in comparison for the calculated changes (solid line).

ESDD
6, 1897–1937, 2015

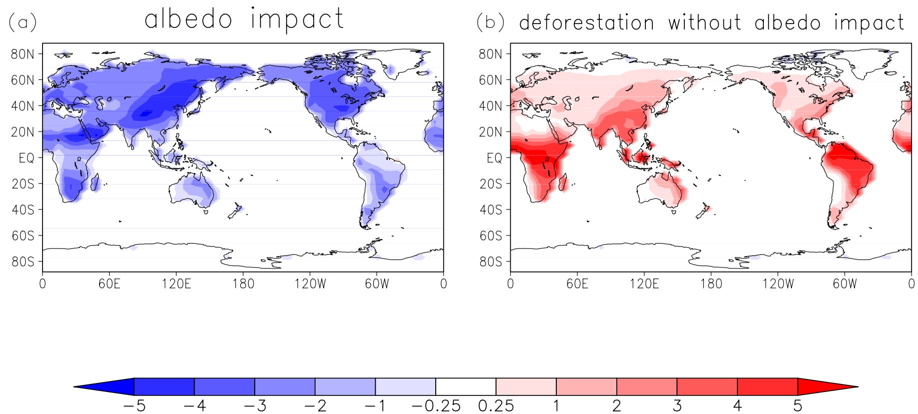

Figure 7. (a) Impact of Albedo (only) on temperature change **(b)** temperature change without albedo impact (K).

ESDD
6, 1897–1937, 2015

Spatial scale and background climate in the latitudinal temperature response

Y. Li et al.

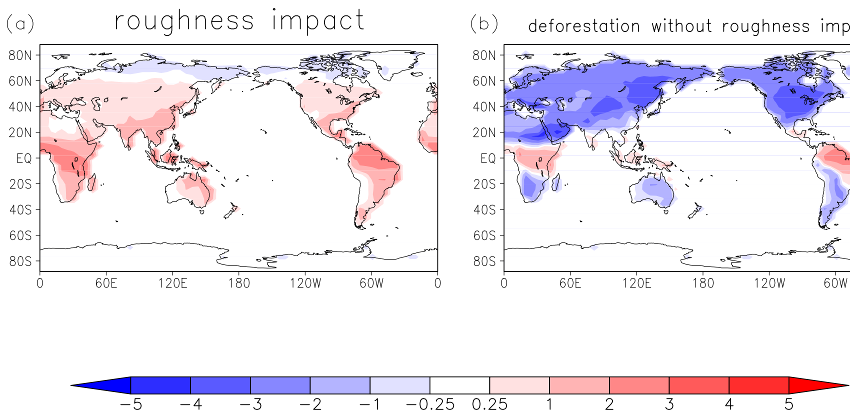

Figure 8. (a) Impact of roughness (only) on temperature (K); **(b)** temperature change without roughness.

ESDD
6, 1897–1937, 2015
Spatial scale and background climate in the latitudinal temperature response
Y. Li et al.

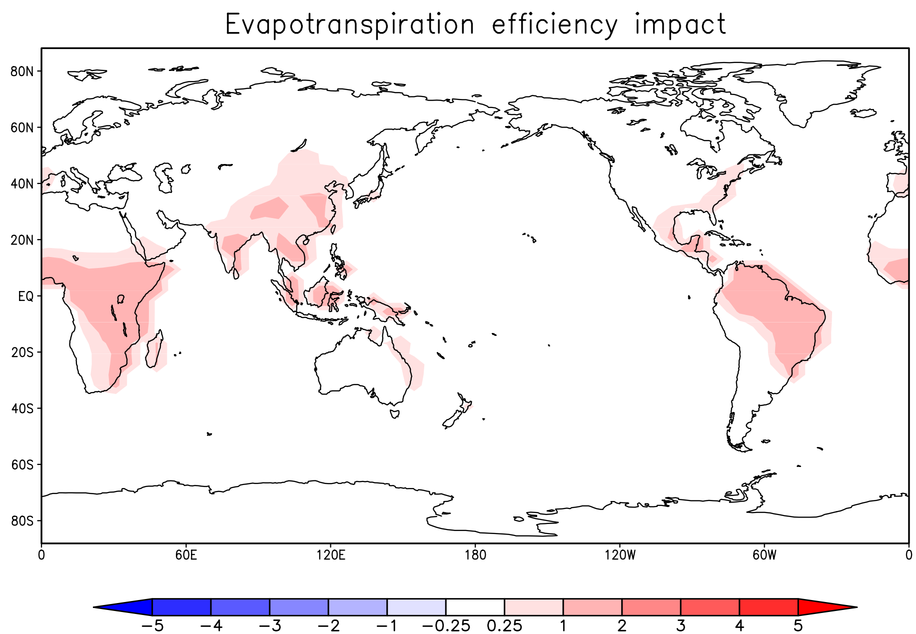

Figure 9. Evapotranspiration efficiency impact on temperature change (K).

ESDD
6, 1897–1937, 2015

Spatial scale and background climate in the latitudinal temperature response

Y. Li et al.

Title Page
Abstract | Introduction
Conclusions | References
Tables | Figures
◀| |▶
◀ ▶
Back | Close
Full Screen / Esc
Printer-friendly Version
Interactive Discussion

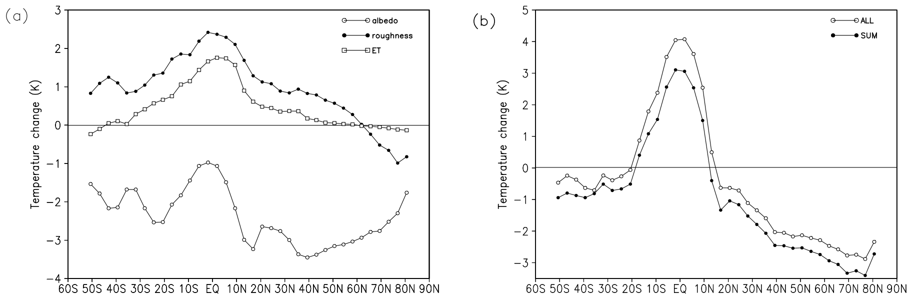

Figure 10. (a) Latitudinal patterns of the contribution of individual biophysical factors to temperature change and **(b)** reconstructed temperature change from individual biophysical effects (SUM = ALL – noALB + ALL – noRGH + EVA – CTL).

ESDD
6, 1897–1937, 2015

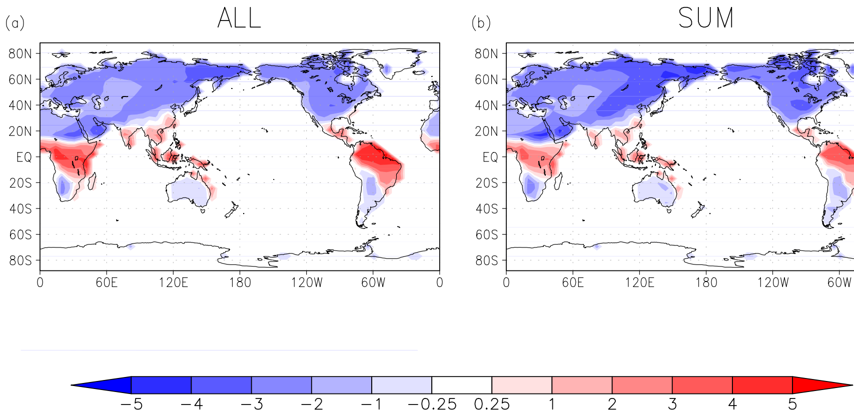

Figure 11. Spatial patterns of **(a)** actual temperature change and **(b)** reconstructed temperature change (SUM = ALL – noALB + ALL – noRGH + EVA – CTL).

ESDD
6, 1897–1937, 2015

Spatial scale and background climate in the latitudinal temperature response

Y. Li et al.

Title Page
Abstract
Introduction
Conclusions
References
Tables
Figures
Back
Close
Full Screen / Esc
Printer-friendly Version
Interactive Discussion